Phase structure of poly(vinyl alcohol) single crystals as revealed by high-resolution solid-state ^{13}C n.m.r. spectroscopy

Shaohua Hu*, Masaki Tsuji and Fumitaka Horii†
Institute for Chemical Research, Kyoto University, Uji, Kyoto 611, Japan
(Received 8 September 1993; revised 26 October 1993)

The phase structure composed of the crystalline and non-crystalline phases, in particular the structure of the non-crystalline phase and hydrogen bonding, has been examined for poly(vinyl alcohol) (PVA) single crystals with different molecular weights by cross-polarization/magic angle spinning ^{13}C n.m.r., differential scanning calorimetry and X-ray measurements. Although the molecular weight is vigorously decreased for the single crystals conventionally prepared from triethylene glycol solution, no reduction in molecular weight occurs when they are crystallized in a triethylene glycol/glycerol mixed solvent after dissolution at relatively low temperatures. According to the method previously reported, the triplets of the CH resonance lines of the crystalline and non-crystalline components have been analysed to obtain information about the intramolecular and intermolecular hydrogen bonds. It is found that the probability of formation of intramolecular hydrogen bonds in the *meso* sequence greatly differs between the crystalline and non-crystalline components, slightly or insignificantly depending on the molecular weight and the crystallization condition. It is finally concluded that PVA single crystals are composed of a crystalline phase with a thickness of about 8.0 nm and a non-crystalline overlayer with a thickness of about 2.0 nm. Moreover, the non-crystalline overlayer should consist of short loops with rather restricted molecular mobility compared to the mobility of the amorphous component.

(Keywords: poly(vinyl alcohol); solid structure; single crystals)

INTRODUCTION

It is well known that lozenge-shaped single crystals with a thickness of about 10 nm are grown when linear polyethylene is crystallized from a dilute solution[1–4]. An early selected-area electron diffraction study clearly revealed that the chain stem of polyethylene is perpendicular to the basal plane of the single crystal as a result of chain folding on the growing lamellar surface. However, the detailed structure of the folding part on the single crystal overlayer is still a controversial subject, probably owing to the scarcity of appropriate analytical methods. We have recently found by high-resolution solid-state ^{13}C n.m.r. spectroscopy that the non-crystalline overlayer of polyethylene single crystals, whose thickness is estimated to be about 2 nm, is composed of relatively short loops with restricted molecular mobility[5]. This region corresponds well to the interfacial region, defined as a transition region between the highly ordered crystalline and completely amorphous regions[6], in the bulk-crystallized polyethylene samples[5,7–9]. A more recent study[10,11] by dark-field electron microscopic imaging has also revealed for edge-on single crystals of polyethylene grown epitaxially on NaCl crystal surfaces that there exist somewhat disordered overlayers with a thickness of about 3 nm which do not contribute to the (002) reflection of the edge-on polyethylene crystals.

In the case of conventional, almost atactic poly(vinyl alcohol), single crystals with a thickness of 10–15 nm are produced when it is crystallized at high temperatures from solutions in polyhydric alcohols such as triethylene glycol[12–15]. The molecular chains with the planar zigzag conformation are also folded perpendicular to the basal plane of the single crystal, but there is no report of the detailed structure of the folding overlayer. In the work described in this paper we have examined the phase structure composed of the crystalline and non-crystalline regions, especially the structure of the overlayer, of poly(vinyl alcohol) (PVA) single crystals as well as the hydrogen bonding in both regions by high-resolution solid-state ^{13}C n.m.r. spectroscopy, as used for the characterization of PVA films or fibres[16–18]. For this purpose we have also developed a modified crystallization method to prepare high molecular weight PVA single crystals without decomposition at high temperatures.

EXPERIMENTAL

Samples

Three types of PVA samples with viscosity-average degrees of polymerization (*DP*) of 1700, 7600 and 15 500, provided by Kuraray Co. Ltd, were used without further purification. The levels of saponification were more than 0.999 for these samples and the triad tacticities determined by gated scalar decoupling ^{13}C n.m.r. spectroscopy in solution were almost the same as the tacticity reported previously for almost atactic PVA[15].

* Present address: Chemical Fiber Research Institute, China Textile University, 1882 West Yan-an Road, Shanghai, People's Republic of China
† To whom correspondence should be addressed

0032-3861/94/12/2516-07

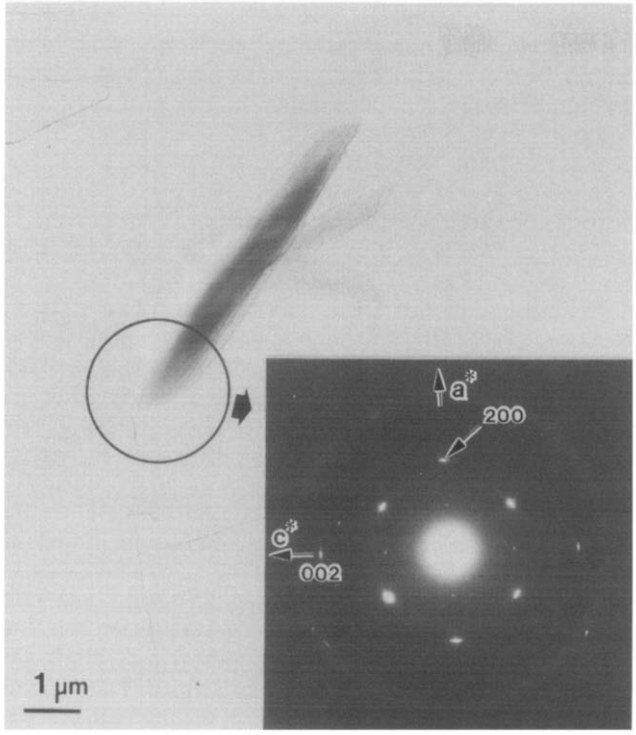

Figure 1 Electron micrograph and the corresponding selected-area electron diffraction pattern for a PVA single crystal prepared from triethylene glycol solution

Preparation of PVA single crystals

A 0.3 wt% PVA solution in triethylene glycol (TEG) was prepared as follows. The dried PVA sample with $DP = 1700$ was immersed in TEG under an atmosphere of argon, heated up to 250°C at a rate of about 3–4°C min^{-1}, and then dissolved for about 1 h by stirring. After complete dissolution, the solution was rapidly cooled to 194°C. Crystallization was carried out by cooling the solution at a rate of 1°C h^{-1}. Alternatively, PVA samples with different molecular weights were also crystallized in a mixed solvent of TEG and glycerol in order to suppress degradation by dissolving them at somewhat lower temperatures (see later). After separation from the crystallization medium with a glass filter, the PVA single crystals were purified by immersing them in methanol at 40°C. The crystals were then dried as a powder at 50°C for about two days under vacuum.

^{13}C n.m.r. measurements

High-resolution solid-state ^{13}C n.m.r. measurements were conducted on a JEOL JNM-FX200 spectrometer operating at a static magnetic field of 4.7 T and equipped with a variable temperature/magic angle spinning (v.t./m.a.s.) system. The detailed procedure has been described in an earlier paper[16]. Each PVA sample was packed into an m.a.s. rotor with an O-ring seal to prevent the absorption of moisture during n.m.r. measurements[16]. ^{13}C chemical shifts were expressed as values relative to tetramethylsilane (Me_4Si) by using the CH_2 line at 32.89 ppm of the orthorhombic crystalline component of polyethylene as an external reference.

RESULTS AND DISCUSSION

Formation of PVA single crystals

Figure 1 shows a transmission electron micrograph and the corresponding selected-area electron diffraction pattern for the PVA single crystals with $DP = 1700$ prepared from the TEG solution. It has been confirmed that the same PVA single crystals are grown in TEG as those previously reported by Tsuboi and coworkers[12,14,15]. Nevertheless, gel permeation chromatography (g.p.c.) revealed for a sample acetylated in an acetic anhydride–pyridine system that the molecular weight of the single crystals is reduced to about one fifth that of the original PVA sample. Since such a vigorous degradation will occur during dissolution at 250°C, we have reduced the dissolution temperature to 185°C by using a TEG/glycerol (1 g/1 g) mixed solvent. After complete dissolution a given amount of TEG was added, keeping the temperature at 193–195°C, and the crystallization was carried out by decreasing the temperature at a rate of 1°C h^{-1}. As a result, it has been confirmed that somewhat longer parallelogram-like single crystals are also produced for PVA samples with different molecular weights in this solvent system. Moreover, almost no reduction in molecular weight has been found for the single crystals by g.p.c. performed after the conversion to poly(vinyl phenyl ether) with phenyl isocyanate. Since the ratio of the length to the width of the single crystals is increased with increasing content of glycerol in accord with an earlier result[19], the final composition (TEG/glycerol) of the mixed solvent was set to be 9 g/1 g in this work in order to obtain better-shaped single crystals.

In *Table 1* are summarized the degrees of crystallinity, long spacings and melting temperatures of PVA single crystals with different molecular weights. Here, the degrees of crystallinity were determined by differential scanning calorimetry (d.s.c.) assuming the melting enthalpy[20] of the PVA crystals to be 6.99 kJ mol^{-1}. The long spacing was determined from a small-angle X-ray scattering pattern, which was obtained as an edge view for several stacked mats of PVA single crystals. These mats were prepared by hot pressing at 181°C under a pressure of 200 kg cm^{-2}. The melting temperature was determined as the peak temperature of the d.s.c. endothermogram. Although the crystallinity is almost the same (0.64–0.67) for all these samples, the long spacing somewhat increases with increasing molecular weight for PVA single crystals prepared in the TEG/glycerol mixed solvent. Such a dependence of the lamellar thickness is also evidently reflected in the change in melting temperature. This fact suggests that thicker lamellae should be grown for a higher molecular weight sample because higher molecular weight PVA will be crystallized at a higher temperature in this solvent system.

Table 1 Degrees of crystallinity, long periods and melting temperatures of PVA single crystals with different molecular weights

Sample	DP^a	TEG/glycerol ratio	x_c^b	L^c (nm)	T_m^d (°C)
SC2P	1 700	10/0	0.635	11.6	230
SC2	1 700	9/1	0.665	11.6	229
SC8	7 600	9/1	0.649	12.1	232
SC16	15 500	9/1	0.666	12.5	237

[a] Viscosity-average degree of polymerization
[b] Degree of crystallinity determined by d.s.c., assuming the heat of fusion for PVA crystals to be 6.99 kJ mol^{-1}
[c] Long period determined by small-angle X-ray scattering for sedimented mats of single crystals
[d] Determined as a peak temperature by d.s.c.

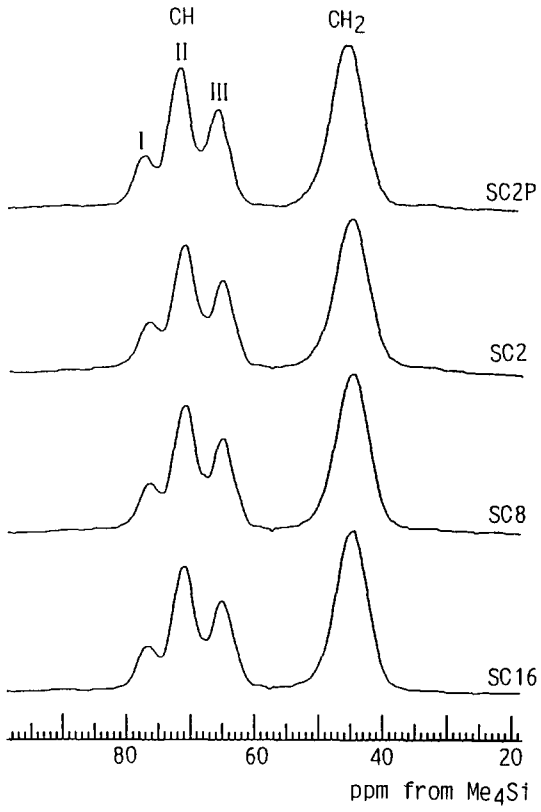

Figure 2 The 50 MHz c.p./m.a.s. ^{13}C n.m.r. spectra of different PVA single crystals at room temperature

Cross-polarization/magic angle spinning (c.p./m.a.s.) ^{13}C n.m.r. spectra

Figure 2 shows the 50 MHz c.p./m.a.s. ^{13}C n.m.r. spectra of different PVA single crystals at room temperature. Here, the contributions from the materials used for the m.a.s. rotor and the probe were removed by subtracting spectra obtained for blank measurements. In accord with the spectra of PVA films with different tacticities[16,21] and atactic PVA fibres[18], the CH resonance splits into three lines (labelled I, II and III) for the respective single crystals. These lines can be assigned to the CH carbons with two, one and no intramolecular hydrogen bonds in the triad sequences in both the crystalline and non-crystalline regions[16–18]. In order to separate the contributions of the crystalline and non-crystalline components, we have examined the ^{13}C spin-lattice relaxation process for these single-crystal samples in detail.

^{13}C spin-lattice relaxation

In *Figure 3* the logarithmic peak intensities of the CH carbon line II, measured at room temperature by the CPT1 pulse sequence[20], are plotted against the decay time for PVA single crystals with $DP = 15\,500$ (SC16). The total decay curve, indicated by open circles, appears not to be described in terms of a single exponential. Similarly to the cases of the films and fibres[16,18], this decay curve was resolved into three components with different spin-lattice relaxation times (T_{1C}), as shown by the dashed lines in *Figure 3*. Since the composite line (solid line) of the three components is in good accord with the observed points, it should be concluded that there exist three components with different T_{1C} values in this sample. By analogy with the case of PVA films[16], the plots with $T_{1C} = 54.0$ s, 12.3 s and 2.9 s are assigned to the crystalline, the less mobile non-crystalline and somewhat more mobile non-crystalline components, respectively. Such a difference in molecular mobility in the non-crystalline components may be due to the difference in conformational freedom. Three similar components were also recognized for the CH_2 resonance line of SC16 and for both the CH and CH_2 lines of other PVA single crystals.

Table 2 lists the T_{1C} values of the CH and CH_2 resonance lines of the various samples, obtained by the CPT1 pulse sequence. Here, only the longer two T_{1C} were measured for SC2P, although a similar component with the shortest T_{1C} was also confirmed qualitatively for this sample. There is no large difference in T_{1C} among the corresponding components but the T_{1C} values of the crystalline components increase slightly with increasing molecular weight for the single crystals prepared in the mixed solvent. This fact seems to correspond to the increases in long period and T_m with increasing molecular weight, as shown in *Table 1*. Since the natural abundance of ^{13}C nuclei is about 1.1%, ^{13}C spin diffusion is normally suppressed to a very low level. Nevertheless, the ^{13}C magnetization of the crystalline region will be relaxed in the non-crystalline region through spin diffusion from the crystalline region to the non-crystalline region when the T_{1C} in the crystalline region is considerably longer than that in the non-crystalline region. Under such circumstances T_{1C} values observed for the crystalline component should be assumed to depend on the size of the crystallites. In fact, it has been found that T_{1C} values are evidently increased with increasing lamellar thickness

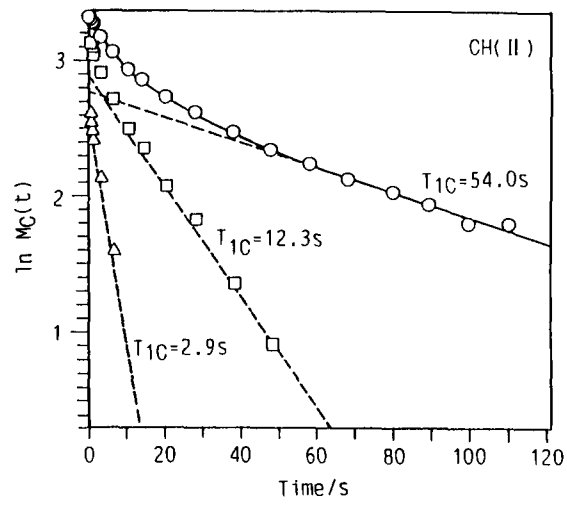

Figure 3 Semilogarithmic plots of the peak intensities ($M_C(t)$) for line II of the CH resonance for PVA single crystals (SC16) as a function of time

Table 2 ^{13}C spin-lattice relaxation times of the various resonance lines of different PVA single crystals, measured at room temperature

Sample	T_{1C}(s) I	II	III	CH_2
SC2P	53.8, 8.0, –[a]	46.5, 8.5, –[a]	50.1, 10.2, –[a]	54.8, 10.4, –[a]
SC2	38.0, 8.8, 1.9	46.0, 10.9, 2.5	45.0, 7.3, 0.9	48.0, 7.1, 1.4
SC8	44.8, 8.0, 2.3	52.0, 10.9, 1.4	53.0, 10.0, 2.0	50.0, 8.7, 0.3
SC16	45.0, 7.1, 0.8	54.0, 12.3, 2.9	50.0, 9.3, 2.2	52.0, 9.5, 1.0

[a] Not measured

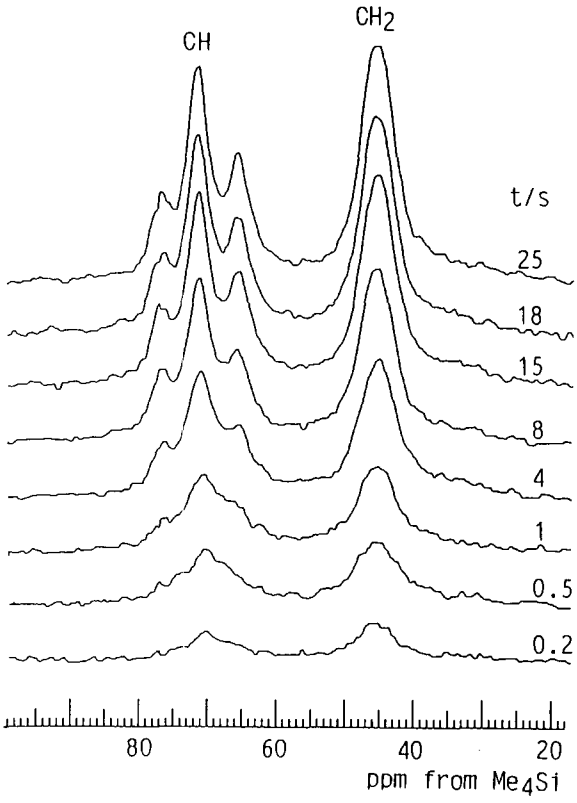

Figure 4 Partially relaxed ^{13}C n.m.r. spectra of PVA single crystals (SC2P) measured at 100°C by the modified saturation recovery method[5,23]

for linear polyethylene samples isothermally crystallized from the melt[5,22]. Accordingly, in the case of PVA the increase in T_{1C} values mentioned above may also be due to the increment in lamellar thickness with increasing molecular weight. This also suggests the existence of some contribution of the ^{13}C spin diffusion to the T_{1C} values in PVA samples.

As described above, the degrees of crystallinity determined by d.s.c. are listed in *Table 1*. Although we tried also to determine the degrees of crystallinity by analysing the ^{13}C spin-lattice relaxation process, it was practically difficult to make precise measurements because of the long T_{1C} values of the crystalline components at room temperature. In this work, therefore, we have analysed the spin-lattice relaxation process at 100°C, where the T_{1C} values of both crystalline and non-crystalline components are significantly reduced by the onset of enhanced molecular motions. However, the cross-polarization (c.p.) efficiencies should be very different in the crystalline and non-crystalline regions owing to the significant difference in molecular mobility between these two regions. This makes the use of the CPT1 pulse sequence[20], which includes the c.p. technique, inappropriate for the precise determination of the degree of crystallinity. We have employed the saturation recovery pulse sequence[5,23] modified for solid-state measurements in this work.

Figure 4 shows partially relaxed ^{13}C n.m.r. spectra of SC2P measured at 100°C by the modified saturation recovery method[5,23], where t is the decay time for the spin-lattice relaxation. In this case the backgrounds from the materials used for the m.a.s. rotor and the probe were removed by subtracting spectra obtained for blank measurements from the observed spectra. As is clearly seen for spectra obtained for $t<1$ s, the CH resonance line seems to be a singlet with a rather broad linewidth. This indicates that there exists a non-crystalline component with a very short T_{1C} in which intramolecular and intermolecular hydrogen bonds are rapidly exchanged or partly broken by the enhanced molecular motion above T_g. In *Figure 5* the integrated intensities of the CH_2 lines shown in *Figure 4* are plotted against decay time t as open circles. These observed points are nicely analysed by assuming the existence of three components with different T_{1C} values. Here, the solid line indicates the composite curve for the three components whose decays are shown as dashed lines. As a result, the fraction of the component with $T_{1C}=35$ s, which corresponds to the component with $T_{1C}=54.8$ s at room temperature shown in *Table 2*, is estimated to be 0.622, in good accord with the degree (0.635) of crystallinity determined by d.s.c. This plot is therefore assigned to the crystalline component. As expected, it is also found that the degree of crystallinity can be determined for PVA by the saturation recovery method, although it may frequently be time consuming. The other two plots should be ascribed to the non-crystalline components. Of these the component with the shortest T_{1C}, which may undergo much enhanced motion, corresponds to the component detected as a broad CH singlet in *Figure 4*, because there also exist three similar components with different T_{1C} values for the CH line. The plot with $T_{1C}=2.4$ s should be simply assigned to the glassy, non-crystalline component, because 100°C is still close to the T_g (70 or 85°C[24]) of PVA.

Spectra of the crystalline and non-crystalline components

Figure 6 shows the CH resonance lines for the crystalline components of the different PVA single crystals, which were selectively measured at room temperature using the CPT1 pulse sequence[20] by setting the delay time[16] to 60 s. In this figure the results of lineshape analyses obtained by a computer-aided least-squares method are also shown. Although an additional contribution must be introduced to line III, the composite curve (dashed line) of lines I, II and III is in good accord with the observed spectrum for each sample. Here, the

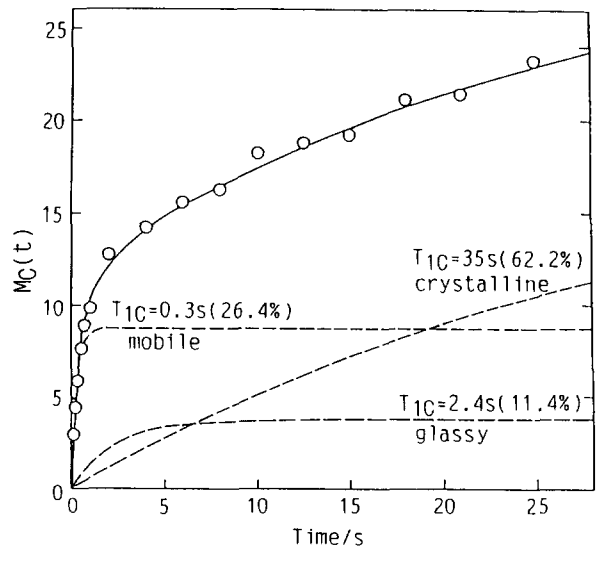

Figure 5 Plots of the integrated intensities ($M_C(t)$) for the CH_2 resonance line shown in *Figure 4* as a function of time: (——) composite curve of the three components obtained by the least-squares method; (– – –) components with different T_{1C} values

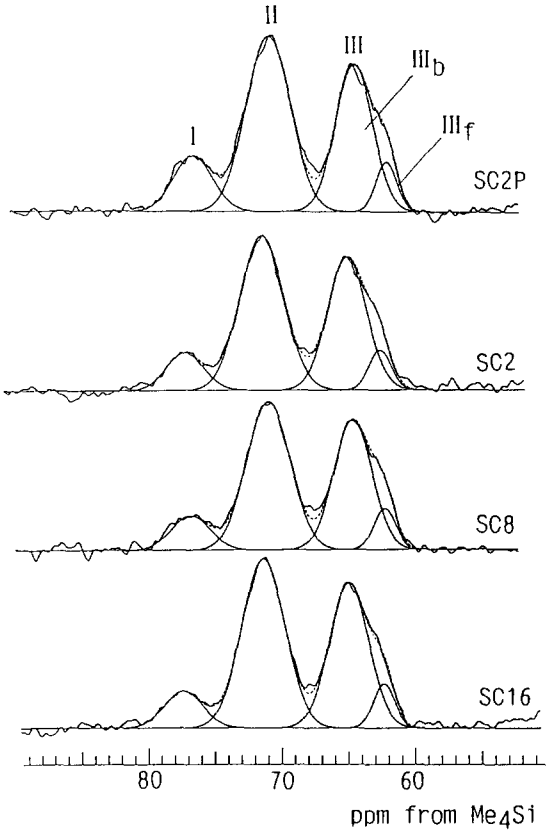

Figure 6 Lineshape analyses for the CH lines of the crystalline components of different PVA single crystals

respective component lines can be assumed to be Gaussian curves. The up-field component of line III, referred to as line III_f, was also observed for the crystalline components in almost atactic PVA films containing some water[16] and in PVA fibres with different draw ratios[18]. According to an earlier assignment, line III_f is assigned to the CH carbon connected to the OH group with no intramolecular or intermolecular hydrogen bonds. Line III_f does not appear for dried PVA films[16] and the fraction of this line is increased for PVA fibres with increasing draw ratio[18]. The existence of line III_f for PVA single crystals suggests, therefore, that some strain may be induced in the crystalline region with the progress of crystallization. On the other hand, the down-field component of line III, designated as line III_b, corresponds to the original line III[16] and thus should be assigned to the CH carbon having the OH group only associated with intermolecular hydrogen bonds.

Figure 7 shows the CH resonance lines of the non-crystalline components for different PVA single crystals, obtained by subtracting the spectra of the crystalline components (*Figure 6*) from the total spectra (*Figure 2*) by use of a previously reported method[16] and using the results of lineshape analyses from the least-squares method. In this case, the composite curves (dashed lines) from lines I, II and III, which are assumed to be Gaussian, are also in good accord with the observed spectra for the respective single crystals. From these results, it is concluded that there is no OH group free from intermolecular hydrogen bonding in the non-crystalline region, because line III_f is not detected for the non-crystalline components of these single crystals.

Table 3 compiles the integrated fractions, chemical shifts and linewidths of the respective components of the CH resonances for the crystalline and non-crystalline components of different single crystals, obtained by the lineshape analyses in *Figures 6* and *7*. The chemical shifts and linewidths almost stay constant irrespective of the crystalline or non-crystalline component for different single crystals. Since the integrated fractions shown in this table contain the effects of the difference in T_{1C} for the respective lines of the crystalline components, the fractions in the non-relaxed state were obtained using the T_{1C} values shown in *Table 2* by a procedure reported elsewhere[16]. Moreover, there is no significant difference in T_{1C} between lines III_b and III_f. It should also be noted here that the relative intensities of the respective resonance lines are almost proportional to chemical composition for spectra of dried PVA samples obtained even by the c.p. method under the conditions employed in this work, as discussed in detail in an earlier paper[16]. In *Table 4* the corrected fractions thus obtained are shown as observed fractions. In addition, the sum of the fractions of lines III_b and III_f is assumed to be the fraction of line III for the further treatment described below.

Table 4 also shows the calculated fractions of lines I, II and III for the crystalline and non-crystalline components of different single crystals, obtained so as to fit the observed fractions by the least-squares method, together with the optimal probabilities p_a for the formation of intramolecular hydrogen bonds in the *meso* sequence and the fractions F_a of OH groups associated with intramolecular hydrogen bonds. In this optimization we used equations previously derived by statistical treatments[17,25] for the formation of the intramolecular or intermolecular hydrogen bond in all possible triad–tetrad and triad–triad pairs in the neighbouring two or three chains on the basis of the crystal structures proposed by Sakurada *et al.*[26] and Bunn[27].

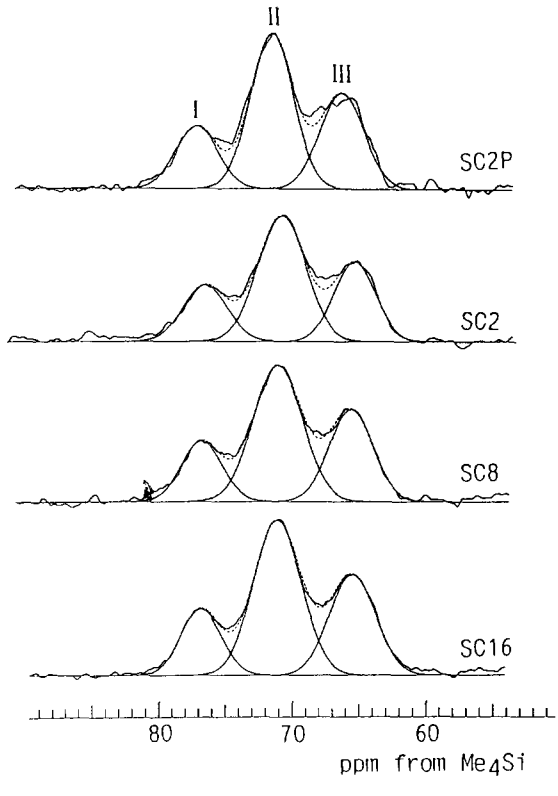

Figure 7 Lineshape analyses for the CH lines of the non-crystalline components of different PVA single crystals

Table 3 Integrated fractions, chemical shifts and linewidths of lines I, II and III of the CH carbons for the spectra of the crystalline and non-crystalline components of different PVA single crystals

	Integrated fraction[a]				Chemical shift (ppm)				Linewidth (Hz)			
Sample	I	II	III_b	III_f	I	II	III_b	III_f	I	II	III_b	III_f
Crystalline												
SC2P	0.131	0.474	0.333	0.062	76.9	71.1	65.0	62.5	172	194	163	91
SC2	0.097	0.477	0.364	0.062	77.2	71.4	65.0	62.5	164	193	171	97
SC8	0.097	0.473	0.364	0.066	76.8	71.0	64.7	62.3	169	190	166	95
SC16	0.093	0.476	0.370	0.061	77.5	71.5	65.0	62.4	169	190	172	93
Non-crystalline												
SC2P	0.195	0.491	0.314		77.0	71.6	66.3		186	188	193	
SC2	0.211	0.510	0.279		76.7	71.0	65.5		195	211	183	
SC8	0.186	0.509	0.305		76.7	70.9	65.5		178	215	191	
SC16	0.181	0.503	0.316		76.8	71.1	65.5		176	209	202	

[a] Uncorrected; for corrected fractions, see *Table 4*

Table 4 Observed and calculated fractions of the CH lines I, II and III for different PVA single crystals

	Observed fraction			Calculated fraction				
Sample	I	II	III	I	II	III	p_a[a]	F_a[b]
Crystalline								
SC2P	0.12	0.50	0.38	0.12	0.50	0.38	0.51	0.38
SC2	0.12	0.46	0.42	0.10	0.48	0.42	0.36	0.35
SC8	0.11	0.47	0.42	0.10	0.48	0.42	0.36	0.35
SC16	0.11	0.45	0.44	0.09	0.46	0.45	0.29	0.34
Non-crystalline								
SC2P	0.22	0.46	0.32	0.16	0.53	0.31	0.87	0.52
SC2	0.21	0.51	0.28	0.18	0.54	0.28	0.98	0.66
SC8	0.17	0.53	0.30	0.17	0.53	0.30	0.91	0.55
SC16	0.16	0.49	0.35	0.16	0.52	0.32	0.80	0.44

[a] Probability for the formation of the intramolecular hydrogen bond in the *meso* sequence
[b] Fraction of OH groups associated with intramolecular hydrogen bonds

Figure 8 shows some examples for the formation of intramolecular and intermolecular hydrogen bonds in the triad–tetrad and triad–triad sequences according to the crystal structure model of Sakurada *et al.*[26]. Here, each arrow indicates the direction of the hydrogen bond involving the OH group. In these cases, the CH carbons in the triads, designated as filled circles, contribute to resonance lines II, III and I in that order from the top to the bottom in *Figure 8*.

The agreements between observed and calculated fractions are quite good for the respective components of different single crystals. The p_a and F_a values are in the ranges 0.29–0.51 and 0.34–0.38, respectively, for the crystalline component. Since $p_a = 0.5$ means that intramolecular and intermolecular hydrogen bonds are equally probable, such low p_a values indicate somewhat preferential formation of the intermolecular hydrogen bonds in the *meso* sequence in the crystalline region. Although there is almost no effect of molecular weight on p_a for the crystalline component, some significant increase in p_a can be recognized for single crystals (SC2P) prepared in TEG compared to p_a for other samples crystallized in the TEG/glycerol mixed solvent.

Such a difference in p_a may be related to the difference in shape of single crystals and then to the difference in growth rates of growing planes in the two solvent systems; as mentioned above, the ratio of the length to the width of parallelogram-like single crystals is larger for the single crystals prepared in TEG/glycerol than for those crystallized in TEG. Since the long and short sides correspond respectively to the (101) and (100) planes, the growth rate of the (100) plane is much higher than that of the (101) plane in the TEG/glycerol solvent compared to the case in TEG. It should therefore be noted that the higher growth rate of the (100) plane may be associated with the smaller p_a value, and thus it may originate from the dominant formation of intermolecular hydrogen bonds perpendicular to the (100) plane. Although the crystal structure of PVA is still a controversial subject, the above discussion supports the model of Sakurada *et al.*[26], where

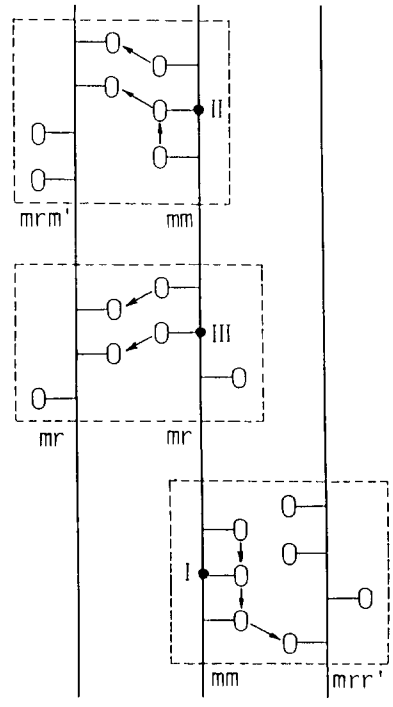

Figure 8 Triad–tetrad and triad–triad pairs which may form intramolecular and intermolecular hydrogen bonds along three PVA chains in the crystalline region in the case of the crystal structure proposed by Sakurada *et al.*[26]: (●) CH carbons associated with the triplet splitting of the c.p./m.a.s. ^{13}C n.m.r. spectrum; (O) oxygen atoms

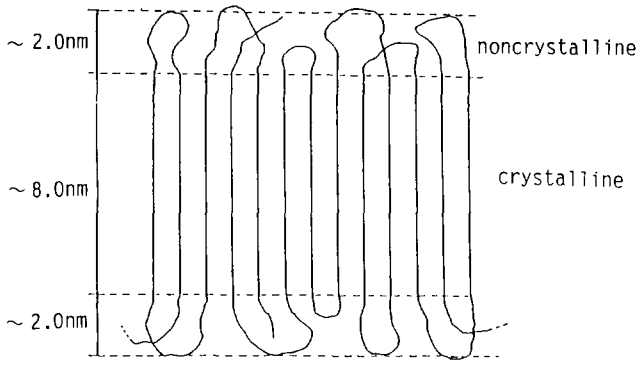

Figure 9 Schematic structure of PVA single crystals

the intermolecular hydrogen bonds are formed almost along the *a* axis.

On the other hand, the p_a values of the non-crystalline components are much higher than those of the crystalline components, being 0.80–0.98. This indicates that the intramolecular hydrogen bonds are predominantly formed in the *meso* sequences in the non-crystalline region. Similar results were also obtained for the non-crystalline components of PVA films[16,17] and fibres[18].

Phase structure of PVA single crystals

On the basis of the results obtained in this work, the schematic structure of PVA single crystals is shown in *Figure 9*. Here, the thicknesses of the crystalline and non-crystalline phases, designated as l_c and l_n, respectively, are calculated from the following equations

$$l_c = Lv_c$$

$$l_n = L(1-v_c)/2$$

where L is the lamellar thickness, which is deduced to be equal to the long period, and v_c is the volume fraction of the crystalline phase. Assuming the densities[24] of the crystalline and non-crystalline phases to be respectively 1.345 and 1.269 g cm^{-3}, the l_c values are estimated to be 7.2–8.2 nm for PVA single crystals, and these are slightly increased with increasing molecular weight for single crystals prepared in the TEG/glycerol system. On the other hand, the thickness of the non-crystalline overlayer is as small as 2.0–2.2 nm for these PVA single crystals. This thickness is almost the same as for polyethylene single crystals[5]. From the model structure of polyethylene single crystals, it should therefore be concluded that rather short loops also form the non-crystalline overlayer for PVA single crystals. Moreover, intramolecular and intermolecular hydrogen bonds are formed in both crystalline and non-crystalline regions, and the probability of formation for the intramolecular hydrogen bond is less than 0.5 in the crystalline region, whereas its probability increases up to over 0.8 in the non-crystalline region.

As shown in *Figures 4* and *5*, the mobile non-crystalline component with $T_{1C}=0.3$ s is observed at 100°C together with the glassy non-crystalline component with $T_{1C}=2.4$ s. However, the former cannot be the rubbery amorphous component, as in the case of polyethylene single crystals. According to the calculation of Flory *et al.*[28], based on the lattice model, the crystalline–amorphous interphase, defined as a transition region between the oriented crystalline region and the completely disordered (amorphous) region, has a thickness of 1.5–2.0 nm for polyethylene. We have also experimentally determined the thickness of the interphase to be about 3.0 nm for polyethylene fractions isothermally crystallized at 130°C from the melt[5]. In the case of PVA, the interphase should not be much thinner compared to polyethylene, although the effect of hydrogen bonds is not quantitatively elucidated yet. Accordingly, the non-crystalline overlayer of PVA single crystals whose thickness is about 2.0 nm seems to be composed of only the interphase, resulting in no appearance of the rubbery amorphous component above T_g. In fact, ^{13}C spin–spin relaxation measurements have revealed that the non-crystalline component does not contain a rubbery amorphous component with a ^{13}C spin–spin relaxation time (T_{2C}) of the order of milliseconds[5]; instead, it contains a less mobile component with T_{2C} less than 100 μs, which corresponds to the interfacial component.

In summary, PVA single crystals consist of a crystalline phase with a thickness of about 8.0 nm and a non-crystalline overlayer with a thickness of about 2.0 nm. The overlayer is composed of relatively short loops folded back to the crystalline phase similar to the non-crystalline region of polyethylene single crystals. Accordingly, the non-crystalline phase of PVA single crystals corresponds to the crystalline–amorphous interphase defined by Flory *et al.*[28], and thus no rubbery amorphous component ever appears above T_g.

REFERENCES

1 Till, P. H. *J. Polym. Sci.* 1957, **24**, 301
2 Keller, A. *Philos. Mag.* 1957, **2**, 1171
3 Fischer, E. W. *Z. Naturforsch., Teil A* 1957, **12**, 753
4 Wunderlich, B. 'Macromolecular Physics', Academic Press, New York, 1973, p. 232
5 Kitamaru, R., Horii, F. and Murayama, K. *Macromolecules* 1986, **19**, 636
6 Flory, P. J., Yoon, D. Y. and Dill, K. A. *Macromolecules* 1984, **17**, 862
7 Zhu, Q., Horii, F., Tsuji, M. and Kitamaru, R. *J. Soc. Rheol., Jpn* 1989, **17**, 35
8 Nakagawa, M., Horii, F. and Kitamaru, R. *Polymer* 1990, **31**, 323
9 Kimura, T., Neki, K., Tamura, N., Horii, F., Nakagawa, M. and Odani, H. *Polymer* 1992, **33**, 493
10 Ihn, K. J., Tsuji, M., Isoda, S., Kawaguchi, A., Katayama, K., Tanaka, Y. and Sato, H. *Polym. Prepr. Jpn* 1989, **36**, 2345
11 Ihn, K. J. PhD Dissertation, Kyoto University, 1990
12 Tsuboi, K. and Mochizuki, T. *J. Polym. Sci. B* 1963, **1**, 531
13 Monobe, K. and Fujiwara, H. *Kobunshi Kagaku* 1964, **21**, 179
14 Tsuboi, K. and Mochizuki, T. *Kobunshi Kagaku* 1966, **23**, 636
15 Tsuboi, K. *J. Macromol. Sci., Phys. B* 1968, **2**, 603
16 Horii, F., Hu, S., Ito, T., Odani, H., Kitamaru, R., Matsuzawa, S. and Yamaura, K. *Polymer* 1992, **33**, 2299
17 Hu, S., Horii, F. and Odani, H. *Bull. Inst. Chem. Res., Kyoto Univ.* 1991, **69**, 165
18 Hu, S., Horii, F., Odani, H., Narukawa, H., Akiyama, A. and Kajitani, K. *Kobunshi Ronbunshu* 1992, **49**, 361
19 Tsuboi, K. and Mochizuki, T. *Kobunshi Kagaku* 1967, **24**, 366
20 Torchia, D. A. *J. Magn. Reson.* 1981, **44**, 117
21 Terao, T., Maeda, S. and Saika, A. *Macromolecules* 1983, **15**, 1535
22 Axelson, D. E., Mandelkern, L., Popli, R. and Mathieu, P. *J. Polym. Sci., Polym. Phys. Edn* 1983, **21**, 2319
23 Hirai, A., Horii, F., Kitamaru, R., Fatou, J. G. and Bello, A. *Macromolecules* 1990, **23**, 2913
24 Sakurada, I. 'Polyvinyl Alcohol Fibers', Marcel Dekker, New York, 1985, p. 115
25 Hu, S. PhD Dissertation, Kyoto University, 1992
26 Sakurada, I., Fuchino, K. and Okada, N. *Bull. Inst. Chem. Res., Kyoto Univ.* 1950, **23**, 78
27 Bunn, C. W. *Nature* 1948, **4102**, 929
28 Flory, P. J., Yoon, D. Y. and Dill, K. A. *Macromolecules* 1984, **17**, 862